processes

MDPI

Article

Semi-Active Vibration Control of Water-Conveying Pipeline Based on Magnetorheological Damper

Sen Pang [1], Xuesong Zhang [2], Zihang Jiang [1], Haixu Yang [3], Shengming Zhou [2] and Qiang Zhao [2,*]

[1] Beijing Building Research Institute Corporation Limited of CSCEC, Beijing 100076, China; eddiejzh@163.com (Z.J.)
[2] College of Mechanical and Electrical Engineering, Northeast Forestry University, Harbin 150040, China; xuesongzhang@nefu.edu.cn (X.Z.); zhoushengming@nefu.edu.cn (S.Z.)
[3] Civil and Traffic College, Northeast Forestry University, Harbin 150040, China
* Correspondence: zhaoqiang@nefu.edu.cn

Abstract: In order to mitigate the vibration caused by fluid–structure interaction in water-conveying pipelines, a semi-active control method based on a magnetorheological (MR) damper is proposed. First, the partial differential equation governing the pipeline micro-element, which is simply supported at both ends, is formulated. This equation is then transformed into state-space expressions through non-dimensionalization and the Galerkin method. Based on passive dissipative control theory, a semi-active control law ensuring Lyapunov global asymptotic stability is derived based on the relative motion between the dynamic vibration-absorbing mass and the pipeline. Next, an on–off control algorithm is designed for the MR damper. The results of simulation and hardware-in-loop experiments demonstrate that the semi-active control law can significantly reduce the vibration of the pipeline system. The contribution of this research is to propose a new MR tuned mass damper (MR-TMD) to suppress vibration in water-conveying pipelines. The proposed MR-TMD scheme and its control method provide a theoretical basis and practical reference for the engineering application of semi-active vibration control in water-conveying pipelines.

Keywords: magnetorheological damper; pipeline; semi-active control; tuned mass damper (TMD)

check for updates

Academic Editor: Gorazd Karer

Received: 15 December 2024
Revised: 9 February 2025
Accepted: 14 February 2025
Published: 18 February 2025

Citation: Pang, S.; Zhang, X.; Jiang, Z.; Yang, H.; Zhou, S.; Zhao, Q. Semi-Active Vibration Control of Water-Conveying Pipeline Based on Magnetorheological Damper. *Processes* **2025**, *13*, 571. https://doi.org/10.3390/pr13020571

Copyright: © 2025 by the authors. Licensee MDPI, Basel, Switzerland. This article is an open access article distributed under the terms and conditions of the Creative Commons Attribution (CC BY) license (https://creativecommons.org/licenses/by/4.0/).

1. Introduction

Water-conveying pipelines are fundamental components of building infrastructure that experience harmful vibration due to water flow pulsation and mechanical equipment vibration. This issue is particularly pronounced in high-rise buildings due to high water pressure and powerful pumping equipment. Prolonged pipeline vibration can lead to several adverse effects. First, it compromises system performance by causing irregular output from the main equipment and affecting their mechanical performance and normal operation. Second, it is worth noting that under the alternating stress caused by vibration, the flange connection bolts of the pipeline may loosen, and the welds joints may crack, potentially leading to water leakage and significant economic losses. Furthermore, in residential buildings, inadequate vibration dampening can allow pump noise from the basement to propagate throughout the pipeline system, causing noise pollution that affects residents' quality of life. Therefore, analyzing pipeline vibration characteristics and developing effective vibration suppression methods are crucial for maintaining the safe and reliable operation of building water supply systems [1].

The vibration suppressing of water-conveying pipelines is linked to the control problem of the fluid–structure coupling system of pipeline structure and water flow [2]. Fluid–structure coupling modeling generally serves as the foundation for analyzing pipeline dynamics and control. Dahmane et al. [3] established an analytical pipeline model with various boundary conditions, completed the numerical fluid–structure interaction analysis using fluid dynamics and finite element analysis software for the structural simulation. Rezaee et al. [4] studied the complex mode shapes, natural frequencies and response of the clamped–clamped pipeline conveying fluid by using fluid–structure interaction and the Timoshenko beam theory. Zhang et al. [5] developed a nonlinear dynamic model for asymmetric boundary pipeline conveying fluid under dual excitation at arbitrary frequencies, and proposed an approximate analytical method for the nonlinear vibration response under multiple excitations at arbitrary frequencies. Alizadeh et al. [6] analyzed the vibration and stability of the fluid-conveying pipeline with stochastic parameters using a Monte Carlo simulation combined with finite element method. Attia [7] employed the finite element method to analyze the free vibration of pipelines conveying fluids and developed a novel algorithm based on Hermitian angles between eigenvectors for the post-processing. Zhao et al. [8] introduced a structural wave propagation method and put forward an improved spectral element method for the analysis of the nonuniform fluid-conveying pipelines.

The aforementioned studies explored model solutions and analyzed the vibration characteristics of water-conveying pipelines from multiple perspectives. Traditional vibration suppression measures used in reducing the vibration of the existing pipeline system basically include optimizing the size and layout of the pipeline during the design period, increasing pipeline constraints, changing the type of pipeline constraints, and reducing the water supply pressure. Although these measures are effective to some extent, they also introduce challenges. For example, increasing pipeline constraints or converting simply supported constraints into fixed constraints can both lead to elevated internal stress within the pipeline. In recent decades, pipeline vibration suppression has primarily been achieved through dynamic vibration absorbers (DVA) [9–12], tuned mass dampers (TMD) [13–15] and nonlinear energy sinks (NES) [16–18]. These methods function by adjusting the natural frequency of the tuned damping mass to match that of the excitation force acting on the pipeline system, utilizing the inertial reaction force of the damping mass to achieve vibration reduction. Philip et al. [16] derived the non-dimensional motion equation for the slow-flow dynamics of a combined pipeline–NES system and investigated the vibration control of a harmonically excited pipeline using a nonlinear damping NES. Aloschi et al. [19] proposed a method to reduce the vibration and impact on a pipeline system periodically supported by rack structures through structural internal damping and nonlinear vibro-impact system. They also introduced a multi-objective optimization design procedure for the vibro-impact system.

Using DVA, TMD, and NES can realize effective vibration suppression, however, they operate within a limited bandwidth near a specific resonance frequency. To address this limitation, the multiple tuned mass dampers (MTMD) method has emerged, which can accommodate a wide distribution of structural natural frequencies [20]. However, the MTMD method requires sufficient TMDs to achieve vibration reduction over a broad frequency range, potentially increasing implementation costs. In recent years, semi-active vibration absorber technology has gained attention, and semi-active TMD offers variable stiffness or damping, inherent stability, and significantly lower power consumption compared to active TMD, while combining the benefits of both active and passive TMD [21]. Semi-active actuation methods include linear electromechanical actuators [22], valve-controlled hydraulic cylinders [23], and magnetorheological (MR) dampers [24]. Weber et al. proposed

a semi-active vibration absorber to mitigate harmonic structural vibration in bridges by using a real-time controlled MR damper [25,26]. Maslanka presented a semi-active tuned mass damper (STMD) for vibration control [27]. The semi-active control force of this STMD is based on a combined acceleration and relative motion feedback. The control parameters are optimized to ensure that the STMD performs equivalently to a passive TMD with up to seven times greater mass. Ghadimi et al. [28] proposed a fuzzy-based controller for the MR damper used in an offshore jacket platform, their controller takes displacement and velocity as input signals and outputs a control voltage to the MR damper. For STMD applications in pipeline vibration, Gong et al. [29] designed a magnetorheological damping clamp and proposed a fuzzy-PID control algorithm to suppress the low-frequency vibrations in hydraulic pipelines.

In summary, the STMD adapts to structural frequency by adjusting variable stiffness and damping. Therefore, it exhibits better vibration suppression performance than the common TMD. At present, research on the semi-active magnetorheological TMD (MR-TMD) for pipeline vibration control remains rarely seen, and an effective semi-active control method for a MR-TMD in fluid–structure interaction pipelines requires further in-depth research. This study aims to address pipeline vibrations caused by both the internal flow velocity and pressure pulsation and the external excitation by establishing a fluid–structure interaction model, and it proposes an effective MR damper-based semi-active control algorithm to suppress vibrations. The novelty and contributions of this paper are as follows:

(1) We established a nonlinear dynamic model of water-conveying pipeline with an MR-TMD, which accounts for both fluid–structure interaction and pipeline-TMD interaction.
(2) We proposed a novel semi-active control algorithm for the pipeline and MR-TMD combined system based on the dissipative control principle in passive control theory, which can solve the expected damping force. We also designed the switch control algorithm to clamp the MR-damper damping force.

This remainder of this paper is organized as follows: Section 2 establishes the analytical models of the water-conveying pipeline and MR damper. It is followed by the design of the pipeline MR-TMD control system, including the overall architecture design and control schemes design in Section 3. Next, Section 4 presents the simulation and hardware-in-loop experiment. Finally, the conclusions of this study are presented in Section 5.

2. Analytical Models

2.1. Model of Water-Conveying Pipeline

A water-conveying pipeline is one of the typical fluid-conveying pipelines, and its dynamic model can be established according to the related theories of fluid-conveying pipelines and fluid–structure interaction theory [30]. Referring to the actual application of a building water-conveying pipeline, this paper selects one section of the water-conveying pipeline with both ends simply supported for analysis. The model is shown in Figure 1. In this figure, x represents the longitudinal coordinate of each point along the length axis of the pipeline, y (or z) is the transverse coordinate describing the transverse vibration of the pipeline, and v is the velocity of the water flow in the pipeline. Consider an infinitesimal section element in the pipeline, which is subjected to bending moments, axial forces, shear forces, damping forces, inertial forces, tangential and normal forces of the water, and gravity.

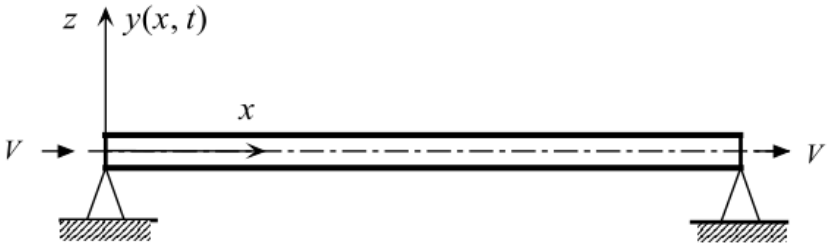

Figure 1. Model of water-conveying pipeline.

According to the fact that the resultant external force in the x direction of the pipeline is zero, the mechanical equation of this infinitesimal section element can be established, and the infinitesimal terms above the second order are all ignored, the partial differential equation of motion of the pipeline is established as follows:

$$\begin{aligned} E^*I\frac{\partial^5 y}{\partial^4 y\partial t}+EI\frac{\partial^4 y}{\partial x^4}+\left(m_fV^2-\overline{T}+\overline{P}A(1-2v\delta)\left(\left(m_f+m_p\right)g+m_f\dot{V}\right)(L-x)\right)\frac{\partial^2 y}{\partial x^2}+\left(m_f+m_p\right)g\frac{\partial y}{\partial x} \\ +2m_fV\frac{\partial^2 y}{\partial x\partial t}+\left(m_f+m_p\right)\frac{\partial^2 y}{\partial t^2}+C\frac{\partial y}{\partial t}+\left((E+E^*\frac{\partial}{\partial t})\frac{A}{2L}\int_0^L y'^2dx\right)\frac{\partial^2 y}{\partial x^2}=0, \end{aligned} \tag{1}$$

where E^* is the dissipation constant of the pipeline material, I is the moment of inertia of the pipeline cross-section, E is the elastic modulus of the pipeline material, m_f and m_p are, respectively, the mass of the water flowing in the pipeline and the pipeline itself, $\overline{T}$ is the axial force on the pipeline, $\overline{P}$ is the pressure of the water flow in the pipeline, C is the viscous damping coefficients, L is the length of the pipeline, g is the gravitational acceleration constant, A is the cross-sectional area of the pipeline, and v is the Poisson's ratio.

In order to realize non-dimensionalization, the following variables and parameters are further defined as follows:

$$\begin{gathered} \eta=\frac{y}{L},\ \zeta=\frac{x}{L},\ \overline{g}=\frac{\left(m_f+m_p\right)gL^3}{EI},\ v=\left(\frac{m_f}{EI}\right)^{1/2}E^*/L^2,\ \beta=\frac{m_f}{m_f+m_p},\ \tau=\left(\frac{EI}{m_f+m_p}\right)^{1/2}t/L^2, \\ \alpha=\left(\frac{I}{E\left(m_f+m_p\right)}\right)^{1/2}E^*/L^2,\ \Gamma=\frac{\overline{T}L^2}{EI},\ \gamma=\frac{AL^2}{2I},\ \mathrm{c}=\frac{CL^2}{\left(EI\left(m_f+m_p\right)\right)^{1/2}}. \end{gathered}$$

By combining the above formulas and Equation (1), the following dimensionless equation can be obtained as follows:

$$\begin{aligned} \alpha\frac{\partial^5\eta}{\partial\zeta^4\partial t}+\frac{\partial^4\eta}{\partial\zeta^4}+\left\{v^2-\Gamma+\Pi(1-2v\delta)+\left(\sqrt{\beta}\frac{\partial y}{\partial t}-\overline{g}\right)(1-\delta)-\gamma\int_0^1\left(\frac{\partial\eta}{\partial\zeta}\right)^2d\zeta-2\alpha\gamma\int_0^1\frac{\partial\eta}{\partial\zeta}\frac{\partial^2\eta}{\partial\zeta\partial\tau}d\zeta\right\}\frac{\partial^2\eta}{\partial\zeta^2}+\overline{g}\frac{\partial\eta}{\partial\zeta}+ \\ 2\sqrt{\beta}v\frac{\partial^2\eta}{\partial\zeta\partial\tau}+c\frac{\partial\eta}{\partial\tau}+\frac{\partial^2\eta}{\partial\tau^2}=0. \end{aligned} \tag{2}$$

The above higher-order partial differential equation is further discretized by using the Galerkin method, and the following Galerkin expansion is used in the discretization process:

$$\eta(\zeta,\tau)=\sum_{r=1}^{N}\varnothing_r(\zeta)q_r(\tau), \tag{3}$$

where ζ is the generalized coordinate, r is the order of the mode shape, and $\varnothing_r(\zeta)$ is the mode function satisfying the boundary conditions. For the simply supported pipeline, the case we studied in this paper, the mode function is

$$\varnothing_r(\zeta)=sin(\lambda_r\zeta), \tag{4}$$

where λ_r is the r-order mode eigenvalue. For the clamped–clamped pipeline, the mode function is

$$\varnothing_r(\zeta)=cosh(\lambda_r\zeta)-cos(\lambda_r\zeta)+\sigma_r(sin(\lambda_r\zeta)-sinh(\lambda_r\zeta)), \tag{5}$$

where $\sigma_r=(\cosh(\lambda_r)-\cos(\lambda_r))/(\sinh(\lambda_r)-\sin(\lambda_r))$.

The discretized low-order differential equation can be obtained by sorting out as follows:

$$\ddot{q} + C\dot{q} + Kq + f(q) + h(q, \dot{q}) = F, \tag{6}$$

where C and K are the linear parts of the equation of motion, and $f(q)$ and $h(q, \dot{q})$ are the nonlinear parts.

The above formula is the complex nonlinear dynamic equation of the pipeline, and the water flows under the fluid–structure interaction state, including the water flow self-excitation of and the external excitation such as water pump. Further the state variables are set as $\mathrm{x} = [x_1, x_2, x_3, x_4]^{\mathrm{T}} = [q_1, q_2, \dot{q}_1, \dot{q}_2]^{\mathrm{T}}$. Equation (6) can be transformed into the first-order differential state equation:

$$\dot{x} = Ax + u(x), \tag{7}$$

where $A = \begin{bmatrix} 0 & 0 & 1 & 0 \\ 0 & 0 & 0 & 1 \\ a_{31} & a_{32} & 0 & a_{34} \\ a_{41} & a_{42} & a_{43} & 0 \end{bmatrix}$, in which $a_{31} = \left(u_0^2 - T - \frac{1}{2}\overline{g}\right)\pi^2 - \pi^4$, $a_{32} = a_{41} = -\frac{40}{9}\overline{g}$, $a_{34} = \frac{16}{3}M_r u_0$, $a_{42} = 4\pi^2\left(u_0^2 - T - g\right) - 16\pi^4$, $a_{43} = -\frac{16}{3}M_r u_0$, $u(x)$ is the control input to the system, and it is as follows: $\begin{pmatrix} u_1 \\ u_2 \end{pmatrix} = \begin{pmatrix} 0 \\ 0 \end{pmatrix}$, and

$$\begin{pmatrix} u_3 \\ u_4 \end{pmatrix} = \mu\overline{B}_1 \begin{bmatrix} x_1 \\ x_2 \end{bmatrix} \omega sin(\omega\overline{\tau}) - \mu\left(\overline{B}_2 \begin{bmatrix} x_1 \\ x_2 \end{bmatrix} - \overline{S}_2 \begin{bmatrix} x_3 \\ x_4 \end{bmatrix}\right) cos(\omega\tau) - \alpha\overline{B}_3 \begin{bmatrix} x_3 \\ x_4 \end{bmatrix} + \begin{bmatrix} Q_1 \\ Q_2 \end{bmatrix} + \begin{bmatrix} F_1 \\ F_2 \end{bmatrix}, \tag{8}$$

where $\begin{bmatrix} Q_1 \\ Q_2 \end{bmatrix} = 2\pi^4\alpha\gamma \begin{bmatrix} c_{11} & 0 \\ 0 & c_{22} \end{bmatrix} \begin{bmatrix} x_1(x_1x_3 + x_2x_4) \\ x_2(x_1x_3 + x_2x_4) \end{bmatrix} + \pi^4\gamma \begin{bmatrix} c_{11} & 0 \\ 0 & c_{22} \end{bmatrix} \begin{bmatrix} x_1\left(x_1^2 + x_2^2\right) \\ x_2\left(x_1^2 + x_2^2\right) \end{bmatrix}$, and F_1 and F_2 are the external excitation.

2.2. Model of Magnetorheological Damper

According to the load and response speed requirements of the water-conveying pipeline, a MR-damper is used as the actuating element for semi-active dynamic vibration absorption. The MR damper uses magnetorheological fluid as the working medium and utilizes the magnetorheological effect to generate real-time adjustable damping force. Specifically, magnetorheological fluid is a special non-gel suspension liquid formed by dispersing and dissolving micro-nano sized hydroxyl iron powder and other easily magnetized particles in insulating carrier liquids such as silicone oil. Under the action of an external magnetic field, the liquid forms a particle chain and enters into a viscoplastic state, thereby generating a controllable damping force on the relative motion of internal and external moving parts of the MR damper. Its response time can reach the millisecond level. Although it exhibits nonlinear hysteresis, it still provides effective damping performance. Considering the amplitude and damping force range of pipeline vibration, this paper proposes to adopt the shear working mode for the MR damper, whose structure is shown in Figure 2.

The dynamics behavior of the magnetorheological damper involves the interaction of several fields such as fluid dynamics, stress–strain, and heat transfer, etc. [31]. The fluid dynamics modeling is based on the Navier–Stokes equation. The flow continuity (namely mass conservation) equation of MR fluid is

$$\nabla u = 0, \tag{9}$$

where ∇ is Del operator. u is flow velocity as shown in Figure 2b.

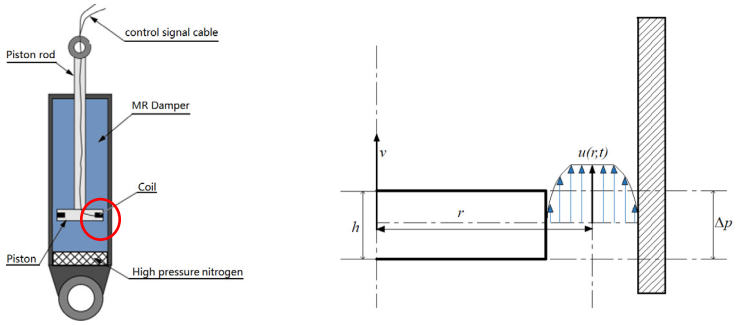

(**a**) (**b**)

Figure 2. Structure and flow model of magnetorheological damper: (**a**) Structure diagram; (**b**) Flow model of through annular gap.

The momentum conservation equation is as follows:

$$\rho\frac{\partial u}{\partial t}+\rho(u\cdot\nabla u)=\nabla p+\nabla\eta\left(\nabla u+(\nabla u)^{T}\right), \tag{10}$$

where ρ is fluid density, p is pressure in flow domain, and η is dynamic viscosity. According to the Bingham model the fluid constitutive equation is as follows:

$$\eta(\dot{\gamma},H(b))=\frac{\tau}{\dot{\gamma}}+\eta_0\ \tau>\tau_y, \tag{11}$$

where $\dot{\gamma}$ is shear train rate, τ is shear stress, τ_y is the yield stress. $H(b)$ is magnetic field strength, and it is the function of magnetic field density b, which is decided by the electrical current of electromagnetic coil.

If the effect of fluid temperature is considered, dynamic viscosity expression of η is given by the modified Bingham model as

$$\eta\left(\dot{\gamma},H(b),T\right)=\left(\frac{\tau_y\tanh(\zeta\gamma)}{\sqrt{\zeta^2+\dot{\gamma}^2}}+\eta_{T_0}\right)\exp(-\lambda(T-T_0)), \tag{12}$$

where T is the absolute temperature.

The transient heat equation for the temperature field in the MR fluid is as

$$\rho C_p\frac{\partial T}{\partial t}+\rho C_p u\cdot\nabla T=\nabla\cdot(k\nabla T)+\tau:\frac{1}{2}(\nabla u+(\nabla u)^{T})-\frac{1}{2}\frac{\partial\rho}{\partial T}\left(\frac{\partial\rho}{\partial t}+(\mathrm{u}\cdot\nabla)p\right)+Q_{\mathrm{t}}, \tag{13}$$

where T is absolute temperature, C_p is specific heat capacity at constant pressure, u is flow velocity, k is heat conductivity, τ is viscous tensor. The rightmost third term at the right side of the formula, i.e., τ: $\frac{1}{2}(\nabla u+(\nabla u)^{T})$, represents the viscous heat of the MR fluid [32], and the rightmost second term represents the pressure work contributing to the heat equation [33]. Q_{t} represents the total external heat coming from the eddy current heating, the hysteresis heating, and inductive heating.

An analytical solution to the above equations cannot be obtained thus far. Generally, some FEA softwares, such us Comsol Multiphysics® (ver 5.0), can be used to attain a numerical solution [34]. After neglecting some terms and the influence of the changes in temperature, the dynamic damping force can be calculated; however, it includes an integral expression, and ultimately, only a numerical solution can be obtained [35].

Additionally, multiphysics behavior analysis and modeling are primarily applied in the design and manufacture stages of MR damper. In this paper, the MR damper model is primarily used for control simulation, where only a simplified analytical model with sufficient accuracy is required. Therefore, a phenomenological model with a limited number

of parameters is more suitable for the rapid requirements of the control simulation. The existing parametric models include the polynomial model, Bingham model, Bouc–Wen model, and others. Some models have been tested and calibrated by experiments and proven to exhibit better accuracy. In this paper, a relatively simpler and more accurate modified Bouc–Wen model [36] is adopted, as shown in Figure 3.

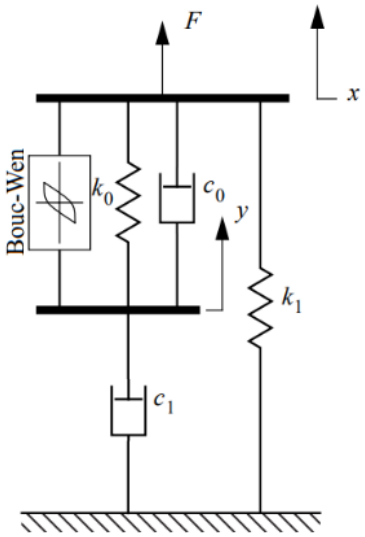

Figure 3. Dynamical damping force model of magnetorheological damper.

The specific modeling process is as follows. The left chain of Figure 3 has the following force relation expression:

$$c_1\dot{y} = \alpha z + k_0(x - y) + c_0(\dot{x} - \dot{y}), \tag{14}$$

where α is a coefficient, c_1 is the viscous damping coefficient at low speed, c_0 is the viscous damping coefficient at high speed, and k_0 is the spring stiffness coefficient at the high-speed stage.

After simplification, we can obtain

$$\dot{y} = \frac{1}{(c_0 + c_1)}[\alpha z + c_0\dot{x} + k_0(x - y)]. \tag{15}$$

The variable z in the above equation is used to describe the Bouc–Wen model:

$$\dot{z} = -\gamma|\dot{x} - \dot{y}||z|z|_{n-1} - \beta(\dot{x} - \dot{y})|z|_n + A(\dot{x} - \dot{y}), \tag{16}$$

where γ, n, β, and A are the model parameters.

Finally, the damping force equation is determined as

$$F = \alpha z + c_0(\dot{x} - \dot{y}) + k_0(x - y) + k_1(x - x_0), \tag{17}$$

where x_0 is the initial displacement, and k_1 is the spring stiffness coefficient in the low speed stage.

Based on Equations (14) and (17), the damping force can be written as

$$F = c_1 y + k_1(x - x_0). \tag{18}$$

When different control voltages are applied in the MR damper coil, the output of the damper will change correspondingly, which is reflected by the fact that some parameters

of the damper are functions of the voltage. Specifically, the parameters related to the output level and the viscous damping constants are all rewritten as the linear functions of intermediate voltage variable v_m as follows:

$$\alpha = \alpha_{0a} + \alpha_b v_m. \tag{19}$$

$$c_0 = c_{0a} + c_{0b} v_m. \tag{20}$$

$$c_1 = c_{1a} + c_{1b} v_m. \tag{21}$$

The specific expression of intermediate voltage variable v_m is

$$\dot{v}_m = -\eta(v_m - u_m), \tag{22}$$

where u_m is the input voltage and η is the response time coefficient.

3. MR-TMD Design

3.1. System Description

The pipeline semi-active damping system with a dynamic vibration absorber based on the magnetorheological damper is designed as shown in Figure 4. The damping part of the dynamic vibration absorber adopts the magnetorheological semi-active damper, which can realize the damping force required by the system by controlling its input current according to the damping requirement of the system. The above dynamic vibration absorber is essentially a common TMD combined with a MR damper and is abbreviated as MR-TMD.

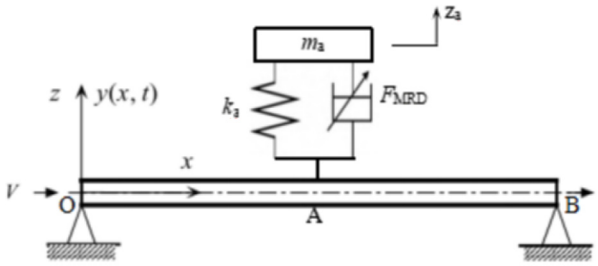

Figure 4. Semi-active damping system for water-conveying pipelines.

Newton's second motion law can be used to establish the equivalent two-degree-of-freedom motion equations of the water-conveying pipeline and the MR-TMD combined system, as follows:

$$m_a \ddot{z}_a + k_a(z_a - z_A) + F_{MRD} = 0, \tag{23}$$

$$\ddot{q} + C\dot{q} + Kq + f(q) + h(q, \dot{q}) = F_{MRD} + k_a(z_a - z_A), \tag{24}$$

where m_a is the dynamic mass of MR-TMD, k_a is the spring stiffness, F_{MRD} is the controllable damping force of the MR damper, and z_A is the displacement of the connection point between the MR-TMD mass and the water-conveying pipeline.

The water-conveying pipeline control system, as shown in Figure 5, adopts a hierarchical control strategy based on state feedback. The upper layer is a system-level controller for the entire pipeline, which is designed using the passive dissipative control method [37]. The displacement and velocity differences (namely errors) are calculated by the system feedback and the expected displacement and velocity. The errors are used as the input to calculate the expected damping force required by the system. The bottom-layer semi-active controller, with the expected damping force as its input, generates a control signal based on semi-active switching algorithm and further sends the control signal to the MR damper, which in turn acts on the pipeline system to achieve effective damping.

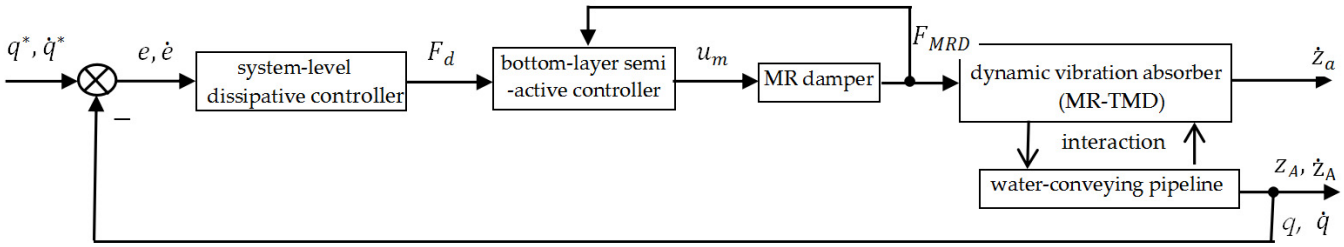

Figure 5. Block diagram of semi-active dissipative control for water-conveying pipelines.

3.2. Control Schemes

Let the desired reference input be q^* as shown in Figure 5, and the error is $e = q - q^*$, then it satisfies the error dynamic equation:

$$\ddot{e} + C\dot{e} + Ke + f(q) + h(q, \dot{q}) = F_d \tag{25}$$

The goal of the system is to make the error and the derivative of the error tend to zero and remain stable, then based on the above equation, let

$$F_d = f(q) + h(q, \dot{q}) - K_p e + v, \tag{26}$$

where K_p is a symmetric positive definite matrix and v is an optional additional control quantity.

Substituting the expression of Equation (26) into Equation (25) results in

$$\ddot{e} + C\dot{e} + Ke + K_p e = v. \tag{27}$$

The energy storage function is taken to be

$$H_e = \frac{1}{2}\dot{e}^T\dot{e} + \frac{1}{2}e^T K_p e. \tag{28}$$

Then, the above energy storage function H_e satisfies the condition of positive definiteness, and in addition, the derivative of H_e satisfies

$$\dot{H}_e = \dot{e}^T\ddot{e} + e^T K_p\dot{e} = -\dot{e}^T C\dot{e} - \dot{e}^T Ke - \dot{e}^T K_p e + e^T K_p\dot{e} \le \dot{e}^T v. \tag{29}$$

Defining the output as $y = \dot{e}$, the $< v, H_e, y >$ system is passive, and the passive feedback component of the system is $f(q) + h(q, \dot{q}) - K_p$e. If the output is defined as $y = \dot{e}$, then $< v, H_e, y >$ system is passive, and the function of the passive feedback component $f(q) + h(q, \dot{q}) - K_p e$ of the system is to shape it into $\frac{1}{2}e^T K_p e$, and meanwhile it has a unique minimum value at $e = 0$. For $v = 0$, there will be $y(t) = 0$, namely $e(t)$ is always equal to 0, then $\ddot{e}(t)$ is always equal to 0, and it can be inferred that $K_p e(t)$ is always equal to 0, namely $e(t)$ is always equal to 0, which indicates that the system is zero-state detectable. Therefore, for any initial value $\varphi(0) = 0$ and for any $y \neq 0$, $y^{\mathrm{T}}\varphi(y) > 0$ always holds true. So, under the control action of $v = -\varphi(\dot{e})$, there exists

$$\dot{H}_e \le \dot{e}^T v = y^{\mathrm{T}}(-\varphi(\dot{e})) = y^{\mathrm{T}}(-\varphi(y)) = -y^{\mathrm{T}}\varphi(\mathrm{y}) < 0. \tag{30}$$

Then, the system is asymptotically stable on a large scale. Therefore, by selecting an appropriate positive definite symmetric matrix K_d, let $v = -K_d\dot{e}$, the final control law of the system can be obtained as

$$F_d = f(q) + h(q, \dot{q}) - K_p e - K_d\dot{e}. \tag{31}$$

The above formula represents the control signal generated by the system-level passive dissipative controller, which is then fed into the bottom-layer semi-active controller to produce the control voltage for the MR damper. Since the magnetorheological damper is a semi-active component, it can generate force only in the required direction during half of the stroke. Therefore, the bottom-layer semi-active controller employs an on–off control algorithm, and the control voltage applied to the magnetorheological damper is as

$$u_m = \begin{cases} sat(kF_d) & if\ F_{MRD}(F_d - F_{MRD}) > 0 \\ 0 & if\ F_{MRD}(F_d - F_{MRD}) \leq 0' \end{cases} \quad (32)$$

where $sat(\cdot)$ is saturation function, and k is the conversion coefficient between the expected damping force and control voltage. F_{MRD} is the actual damping force output by the MR-damper.

4. Simulation and Experiment Test

4.1. Numerical Simulation

The pipeline parameters are set to: E = 1.0 × 10^9 pa (resin material), I = 9.59 × 10^{-5} m^4, m_p = 30 kg, m_f = 70 kg, $\overline{P}$ = 7.5 × 10^5 Pa, ω = 30, μ = 0.4. The MR damper parameters are $c_{0a} = 2100\ N \cdot s \cdot m^{-1}$, $c_{0b} = 350\ N \cdot s \cdot m^{-1} \cdot V$, $c_{1a} = 28{,}300\ N \cdot s \cdot m^{-1}$, $c_{1b} = 295\ N \cdot s \cdot m^{-1} \cdot V$, $\alpha_a = 14{,}000\ N \cdot m^{-1}$, $\alpha_b = 695\ N \cdot m^{-1} \cdot V$, $\eta = 190\ s^{-1}$. According to the above Figure 5, the simulation model of the semi-active damping system of the whole water-conveying pipeline is established with Matlab (2019a) Simulink toolbox [38] as shown in Figure 6. In this figure, the far-right two "Scope" blocks labeled "Displacement" and "velocity" represent the displacement and velocity response outputs, respectively. The "Displacement" block includes three routes of displacement input signals that come from "Pipeline without TMD" model, "Pipeline with TMD" model and "Pipeline with MR-TMD" model, respectively, and similar arrangement also can be found at the "velocity" block. All the above displacements and velocities refer to the displacement and velocity of point A on the pipeline.

By running the above simulation model, the free vibration of the system under initial displacement excitation and the forced vibration under external sinusoidal excitation are simulated. The external sinusoidal excitation is used to simulate the vibration response of the pipeline system caused by the periodic oscillations of the water-supplying pump. First, the pipeline length (i.e., the distance between two simply supported fixed points, also called span) is set to 3.9 m, and the flow velocity is set to 1 m/s. The input voltage is set to a fixed values of 0.2 V when $F_{MRD}(F_d - F_{MRD}) > 0$, and the simulation result is presented in Figure 7. In this figure, Z_A represents the vibration displacement of position point A on the pipeline, and V_A is the vibration velocity of this point. To verify the performance of the MR-TMD, the vibration responses of the systems without TMD and with a general TMD, respectively, are also simulated and depicted in these figures.

The vibration displacement and velocity in Figure 7 is relatively large, and the length of the pipeline has been further shortened to 3 m, and the proposed control method in Equations (31) and (32) is used. The water flow velocity is set to be 2.5 m/s, the simulation results are presented in Figure 8.

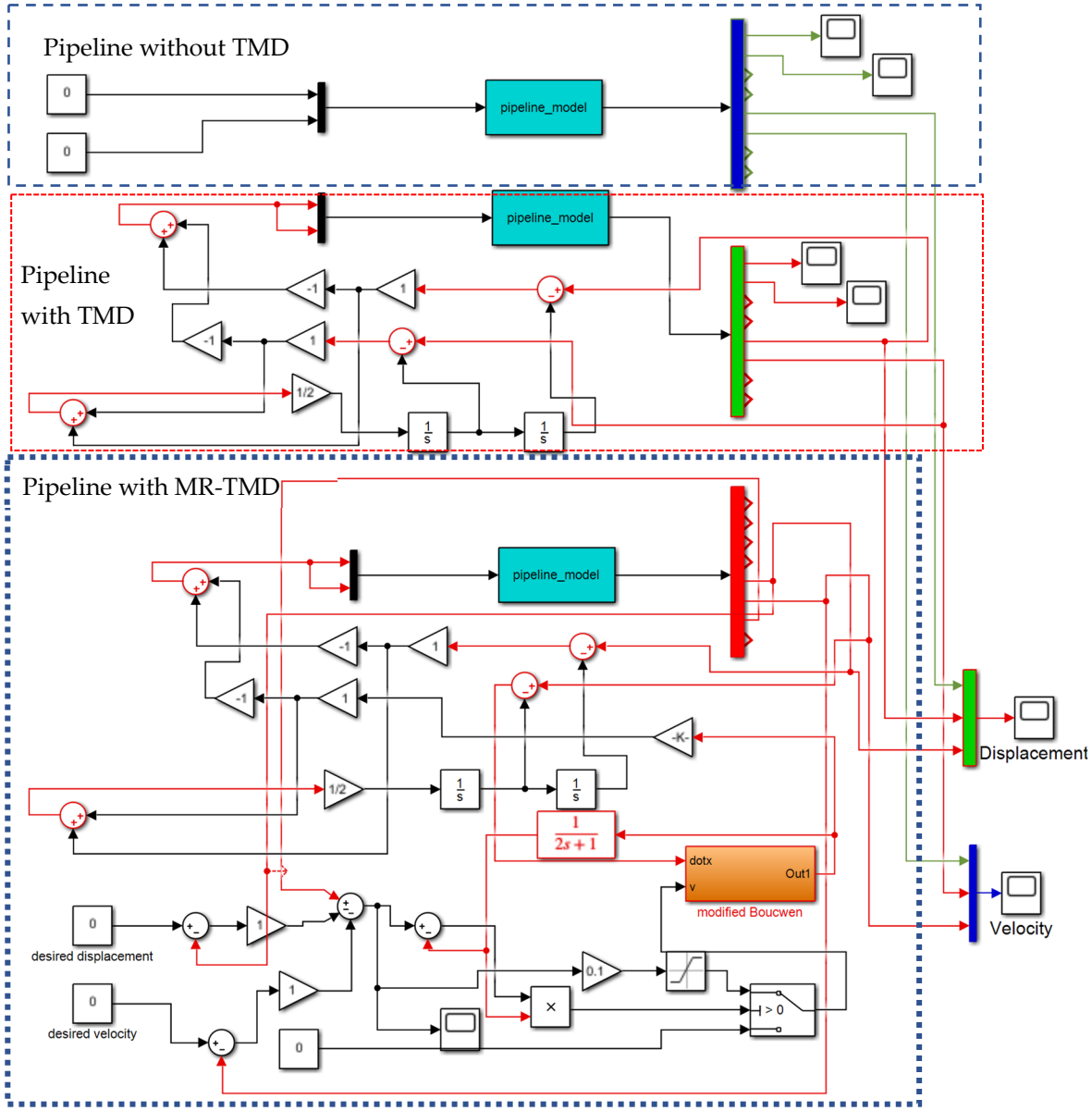

Figure 6. Simulation model of pipeline vibration control system.

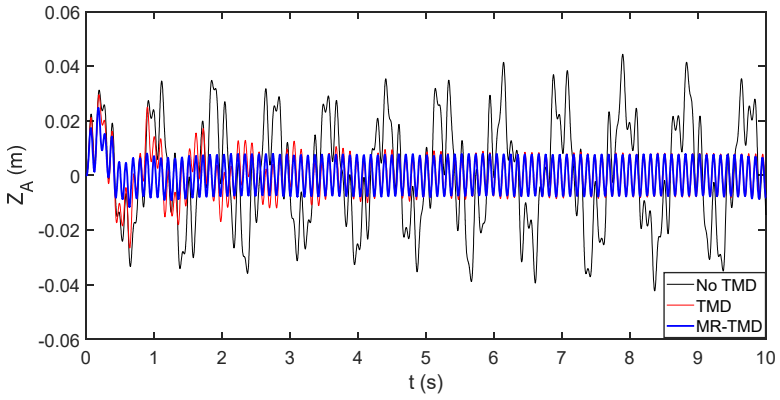

(**a**)

Figure 7. *Cont.*

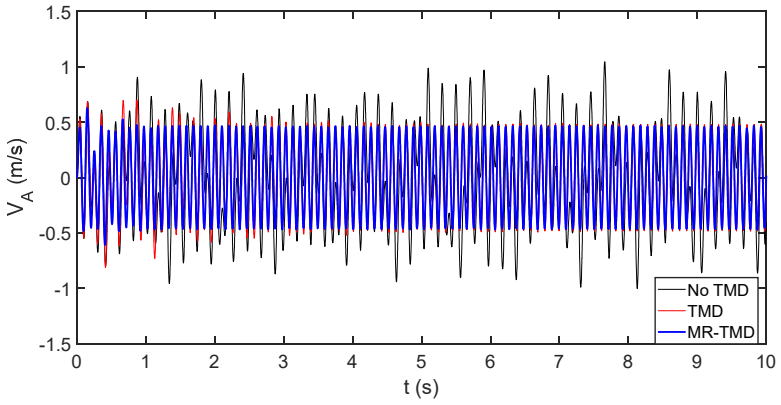

(**b**)

Figure 7. Vibration response with pipeline with length of 3.9 m and fixed-value on–off control: (**a**) Displacement; (**b**) Velocity.

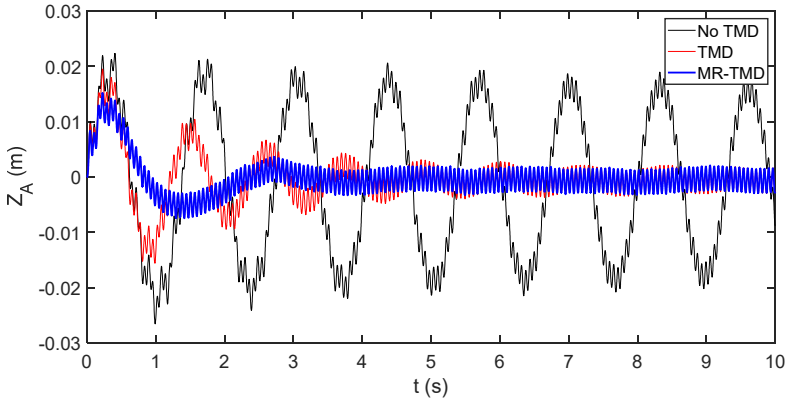

(**a**)

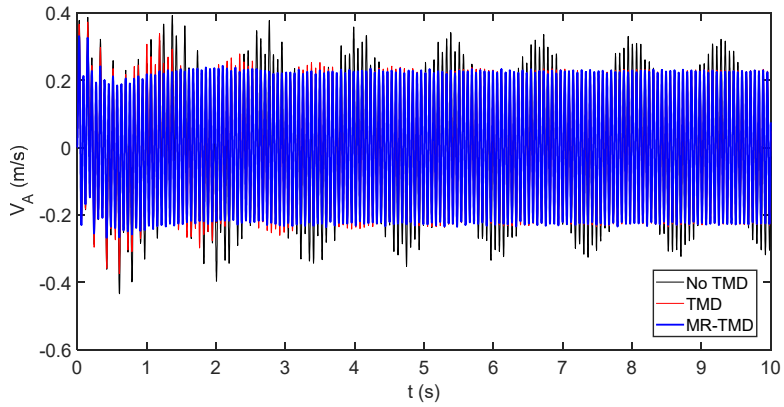

(**b**)

Figure 8. Vibration response with external excitation under $L = 3$ and $v_f = 2.5$ m/s: (**a**) Displacement; (**b**) Velocity.

Removing the external excitation, an initial displacement of 0.02 m both for q_1 and q_2 is exerted on the first two-mode coordinates with the other parameters setting unchanged, the free vibration response with initial displacement is shown in Figure 9.

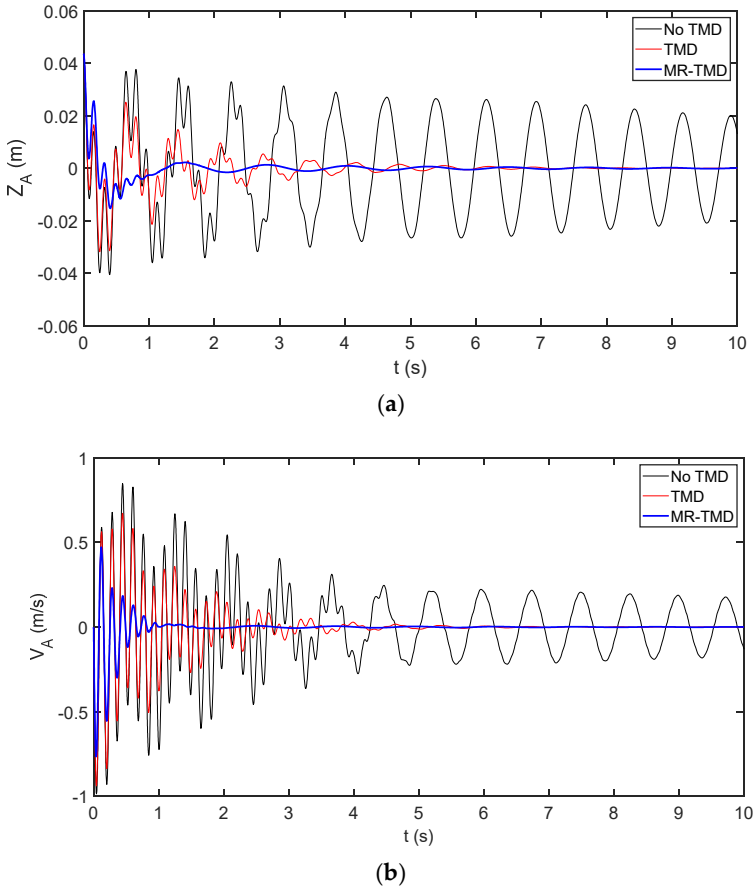

Figure 9. System free vibration response with initial displacement: (**a**) Displacement; (**b**) Velocity.

It can be inferred from Figures 8 and 9 that the control effect of MR-TMD is better than both those without TMD and with a common TMD. Both the vibration displacement and vibration velocity of the feature points are significantly reduced. Summarizing the results from Figures 8 and 9, the maximum of the absolute values of displacements and velocities (namely max (abs(Z_A)) and max (abs($\dot{Z}_A$)) of the three methods (No TMD, TMD and MR-TMD) are presented in Tables 1 and 2. It is noted that for the free vibration case the three displacement curves have the same initial value, so the second peak values (at about t = 0.4 s) are taken for comparison.

Table 1. Displacement response values of pipeline systems with three damping methods under two cases.

Case	Displacement Response (m)				
	No-TMD	TMD	MR-TMD		
			Response Value	Improved Value Relative to No-TMD	Improved Value Relative to TMD
External excitation	0.0265	0.0195	0.0152	42.6%	22.1%
Free vibration	0.0405	0.0318	0.0153	62.2%	51.9%

It can be seen from Tables 1 and 2 that the maximum improvement achieved by MR-TMD compared to the other two methods can reach 62.2%. The least improvement still reaches 11.6%. The decreasing in displacement vibration amplitude by using MR-TMD effectively prevents the looseness of the components in the pipeline.

Table 2. Velocity response values of pipeline systems with three damping methods under two cases.

Case	Displacement Response (m)				
	No-TMD	TMD	MR-TMD		
			Response Value	Improved Value Relative to No-TMD	Improved Value Relative to TMD
External excitation	0.4346	0.3744	0.3310	23.8%	11.6%
Free vibration	0.9860	0.9382	0.7652	22.4%	18.4%

The simulation results with a pipeline length of 3 m demonstrate a satisfactory vibration attenuation effect. Furthermore, the pipeline length was further reduced to 1.5 m, and a simulation under the same external excitation is conducted, with the results presented in Figure 10.

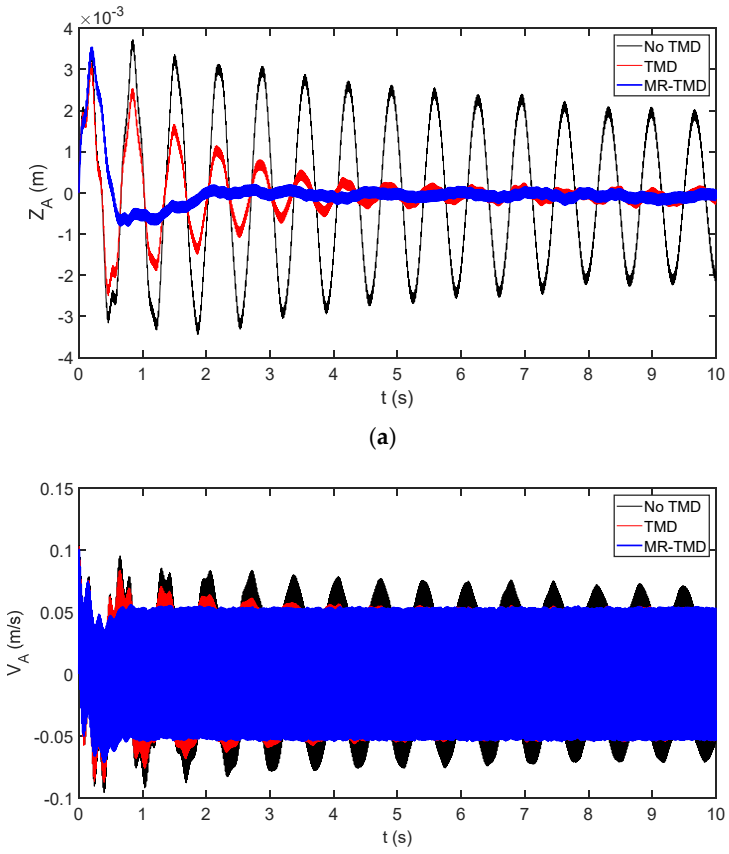

Figure 10. Vibration response with external excitation under L = 1.5 m and v_f = 1 m/s: (**a**) Displacement; (**b**) Velocity.

It can be seen from Figure 10 that the vibration attenuation is further enhanced. However, a shorter pipeline length, i.e., a shorter distance between two simply supported ends, necessitates additional pipeline supports, leading to increased costs. Therefore, a pipeline length of 3 m is considered more suitable. Furthermore, for a pipeline length of 3 m, its ability to suppress vibrations caused by the water hammer effect is further investigated. The simulated water pressure fluctuation due to the water hammer effect is presented in Figure 11a, based on the findings in [39]. The pipeline initially operates at a normal pressure of 7.5 bar, and at 4.5 s, the pressure begins to oscillate for approximately 2–3 s. The simulation results are shown in Figure 11b,c. Under the influence of the water

hammer effect, the displacement response shows a significant increase in the No-TMD case, while it remains nearly unchanged in the MR-TMD case.

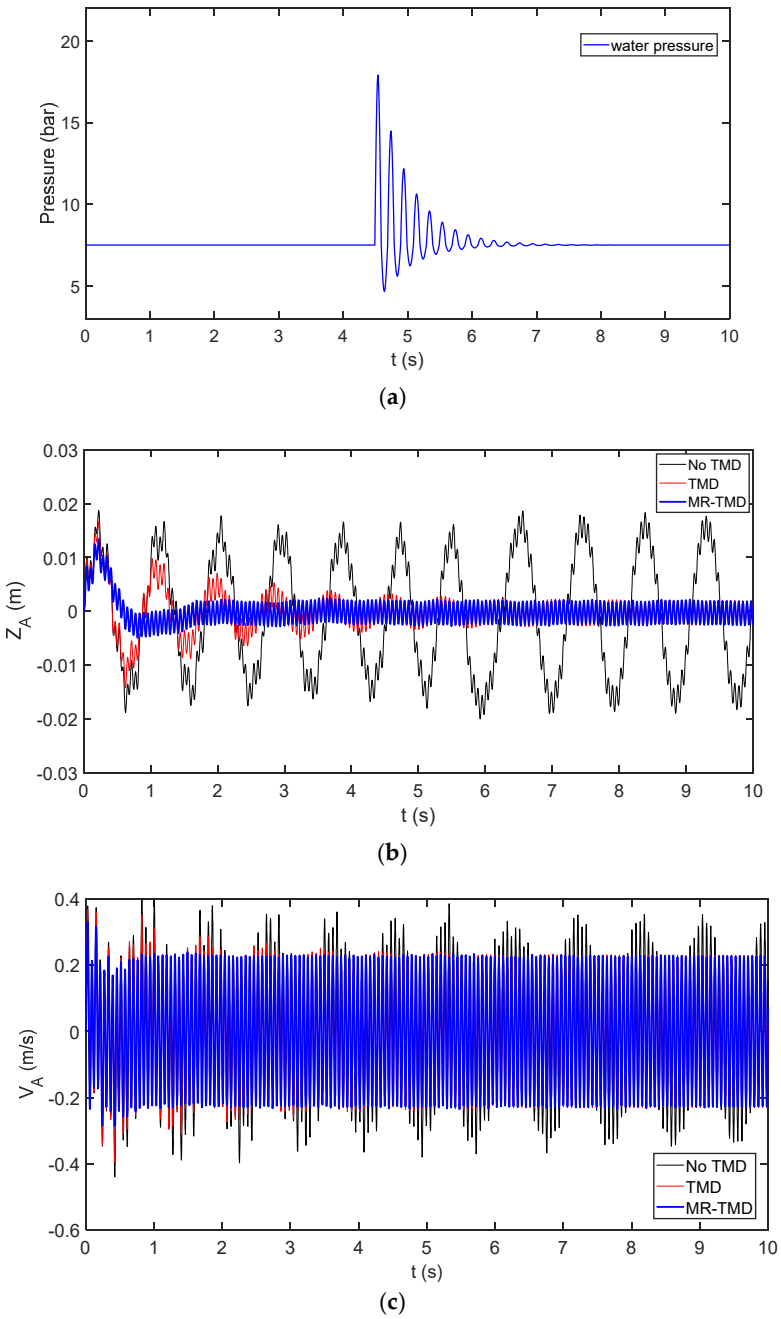

Figure 11. Vibration response under impact caused by water hammer effect: (**a**) Significant fluctuations in water pressure; (**b**) Displacement; (**c**) Velocity.

4.2. Hardware-in-Loop Experiment

According to the above control method, a hardware-in-loop (HIL) simulation test bench for semi-active vibration control on a fluid–structure interaction pipeline is set up, as shown in Figure 12. The control model is implemented using the Matlab Real-Time Workshop (RTW) system. Figure 12d is the monitor for display and monitoring purposes when conducting experiments.

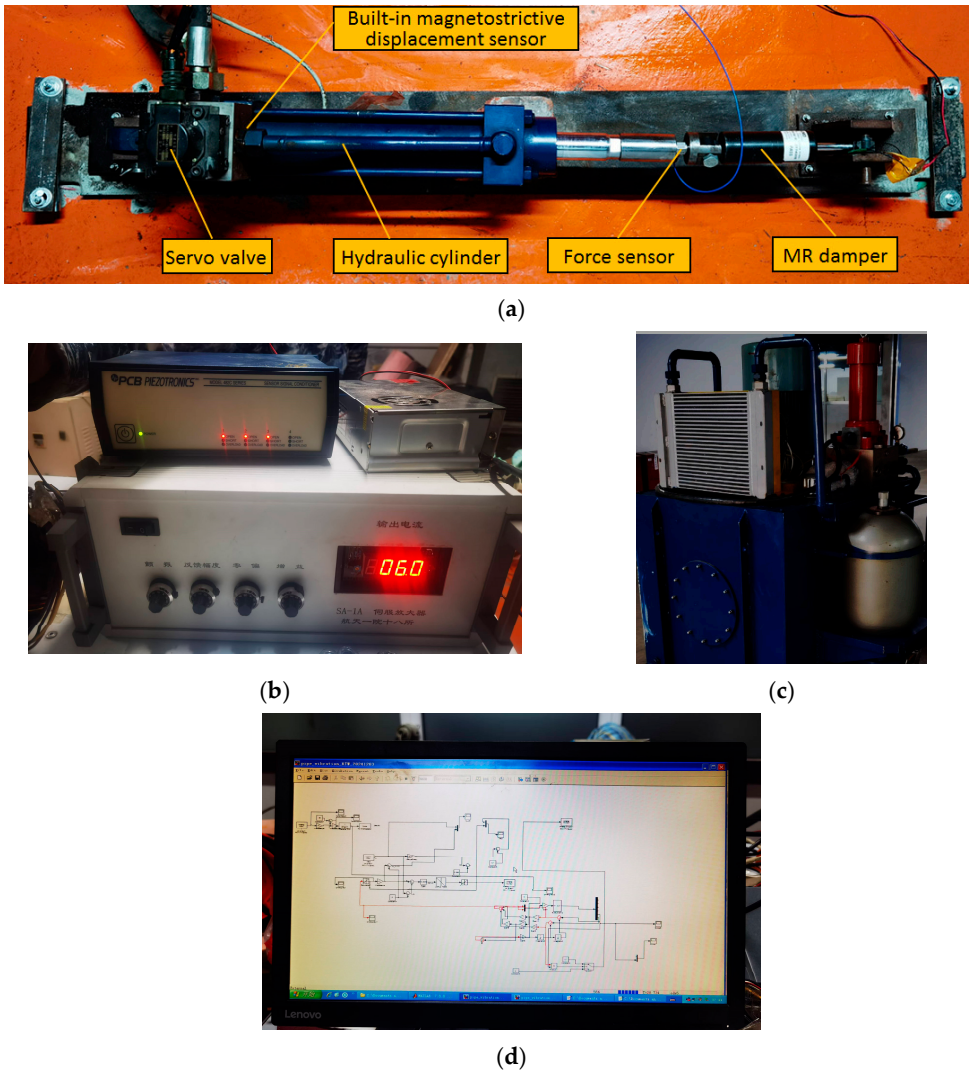

Figure 12. Hardware-in-loop experimental bench for semi-active vibration reduction system: (**a**) Main part of the test bench; (**b**) Force sensor signal conditioner and hydraulic servo amplifier; (**c**) Hydraulic power unit; (**d**) Monitor.

The control hardware comprises a valve-controlled servo cylinder, an MR damper, a force sensor, and a displacement sensor. The MR damper serves as the actual hardware and is actuated by the cylinder, which is controlled by a servo valve. The sensors interact with a fluid–structure coupling model in the control computer in real time, enabling hardware-in-loop (HIL) simulation in continuous running.

As shown in Figure 13, the fluid–structure interaction model in the control computer generates the displacement of the MR damper through real-time running, transmits a displacement signal for the valve-controlled cylinder, and this displacement signal serves as the expected displacement. The valve-controlled cylinder moves according to the expected displacement signal to drive the MR damper to expand and contract generating a corresponding damping force. This damping force is measured by the force sensor and transmitted back to the fluid–structure interaction model, and the fluid–structure coupling model further updates to a new state. So, the real-time hardware-in-loop simulation is continuously carried out.

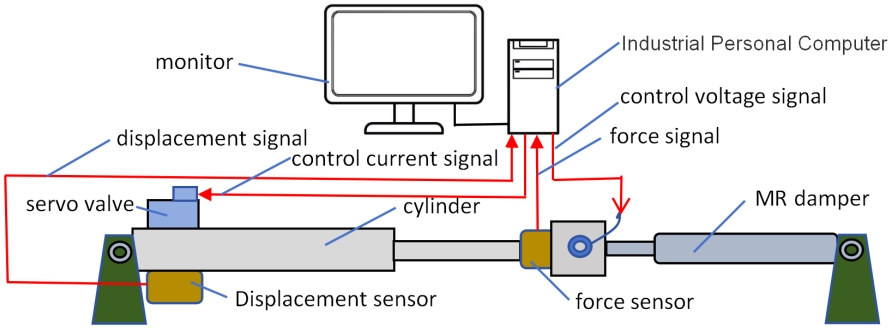

Figure 13. Structure and signal flow of the hardware-in-loop test bench.

The parameter values of the experimental control model are set according to the simulation case, and the experimental test is conducted under the condition of external sinusoidal excitation and by a fixed-value on–off control for MR damper. The vibration displacement and velocity of the pipeline are obtained as shown in Figure 14.

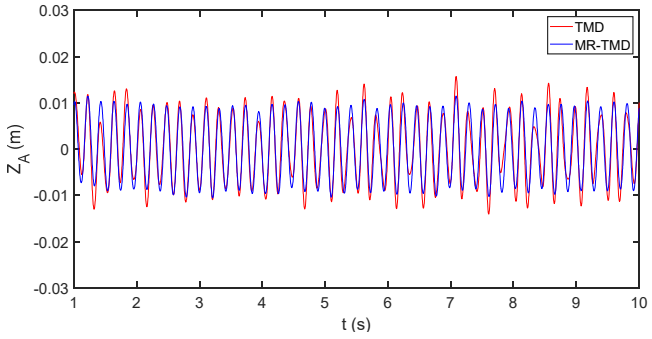

(**a**)

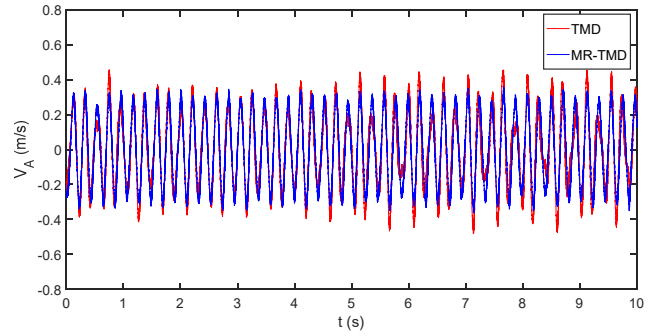

(**b**)

Figure 14. Result of MR-TMD HIL experiment: (**a**) Displacement curves; (**b**) Velocity curves.

From Figure 14, we can conclude that using MR-TMD the vibration displacement of the pipeline feature points is basically between ±0.01 m, the vibration velocity is mostly between ±0.4 m/s, and MR-TMD has better effect than the TMD case, which further demonstrates the effectiveness of MR-TMD.

4.3. Discussion

The above simulations investigate the three cases of pipeline length, being 3.9, 3, and 1.5 m, respectively, which also means the three different spans of the same pipe. As evidenced in Figures 7, 8 and 10, excessive spans led to unacceptably large vibrations that would be impractical for actual pipeline installations. In addition, the results clearly demonstrated that vibration amplitude diminished significantly as the span length was

reduced. However, it should be noted that overly small spans would require additional pipeline supports, resulting in higher installation costs. Based on these considerations, the moderate span length of 3 m was selected for further study.

A thorough analysis of Figures 8 and 11 revealed that external excitation had a markedly greater influence on pipeline vibration compared to internal factors such as water-flow velocity and pressure pulsation. Compared with the case without TMD and relying solely on the supports at both ends for vibration reduction, the introduction of TMD can significantly reduce the vibration of pipeline. The further introduction of the MR damper into TMD (namely MR-TMD) enhances the vibration suppression effect. Although the damping effects of TMD and MR-TMD tend to be consistent after the vibration enters steady-state phase, pipelines using MR-TMD have smaller vibration amplitudes in the transient-state phase, which can be seen from Figures 7–11. When considering that the large amplitude and impact during the transient phase are more likely to cause damage to the pipeline, MR-TMD has practical value and significance.

The enhanced performance of the MR-TMD system can be attributed to two principal mechanisms: First, it can effectively use the unified passive dissipative control algorithm to obtain an effective damping force (F_d) based on the relative motion state between TMD mass and the pipeline. Second, the bottom-layer semi-active controller can further figure out the control quantity to make the MR damper track F_d, which is possible via the on–off control algorithm. The superior vibration attenuation capabilities of the MR-TMD system, compared to conventional TMD system, were conclusively validated through HIL experiments.

5. Conclusions

The mathematical model of transverse vibration in a fluid–structure interaction with water-conveying pipelines is first established. Next, a semi-active control algorithm for the MR damper is derived based on passive dissipative control theory. Finally, the effectiveness of the algorithm is validated through simulation and experimentation. The conclusions are as follows:

(1) The control law based on passive dissipative control theory is theoretically proven to be inherently stable and capable of determining the expected damping force effectively. Besides the control terms related to the error and its variation, the additional compensation terms play an important role in suppressing disturbances.

(2) The proposed MR-TMD demonstrates superior performance, achieving a maximum improvement of 62.2% in vibration suppression compared with the case without TMD, indicating that MR-TMD is highly applicable in practical scenarios. Although introducing MR dampers in practical TMD applications may initially increase costs, mass production for long pipelines can reduce costs. Additionally, the extremely low power consumption of MR dampers ensures a minimal impact on operating costs. Amortizing the purchase and operating costs of MR dampers into the construction and long-term operating costs of each pipeline section can minimize the overall cost impact on the pipeline system.

(3) The proposed control algorithm exhibits global asymptotic convergence characteristics and maintains effective control performance, even when the system undergoes a water hammer impact.

These findings strongly indicate that the proposed vibration suppression method is more effective, successfully meeting the objectives of this study. Future works could explore optimizing fluid transport through circular pipelines and developing a semi-active MR-TMD prototype for practical pipeline vibration reduction, followed by experimental validation.

Author Contributions: Conceptualization, S.P. and Q.Z.; data curation, H.Y.; formal analysis, Q.Z.; funding acquisition, S.P.; investigation, Z.J.; methodology, Z.J.; project administration, S.P. and Z.J.; software, X.Z. and Q.Z.; supervision, S.P. and Z.J.; validation, Z.J., H.Y. and S.Z.; visualization, Z.J., S.Z. and Q.Z.; writing—original draft, X.Z. and Q.Z.; writing—review and editing, X.Z. and Q.Z. All authors have read and agreed to the published version of the manuscript.

Funding: This research was funded by CSCEC-PT-015 CSCEC City Renovation and Intelligent Operation Engineering Research Center (Building Health Diagnosis and Treatment).

Data Availability Statement: The data presented in this study are available on request from the corresponding author.

Conflicts of Interest: Authors Sen Pang and Zihang Jiang were employed by the company Beijing Building Research Institute Corporation Limited of CSCEC. The remaining authors declare that the research was conducted in the absence of any commercial or financial relationships that could be construed as a potential conflict of interest.

References

1. Tang, Y.; Zhang, H.J. Recent progress on dynamics and control of pipes conveying fluid. *Nonlinear Dyn.* 2024, *early access*. [CrossRef]
2. Hicham, F.; Abdelhamid, H. A new fluid-structure coupling model: Case of a pipe under internal pressure. *Adv. Mech. Eng.* **2023**, *15*, 168781322311761. [CrossRef]
3. Dahmane, M.; Boutchcha, D.; Adjlout, L. One-way fluid strucutre interaction of pipe under flow with different boundary conditions. *Mechanika* **2016**, *22*, 495–503.
4. Rezaee, M.; Maleki, V.A. On the complex mode shapes and natural frequencies of clamped-clamped fluid-conveying pipe. *Appl. Ocean Res.* **2024**, *150*, 104113. [CrossRef]
5. Zhang, J.N.; Ding, H. Multi-frequency harmonic balance method for nonlinear vibration of pipe conveying fluid under arbitrary dual-frequency excitation. *Nonlinear Dyn.* 2024, *early access*. [CrossRef]
6. Alizadeh, A.A.; Mirdamadi, H.R.; Pishevar, A. Reliability analysis of pipe conveying fluid with stochastic structural and fluid parameters. *Eng. Struct.* **2016**, *122*, 24–32. [CrossRef]
7. Attia, S.; Mohareb, M. Finite element analysis for free vibration of pipes conveying fluids–physical significance of complex mode shapes. *Thin-Walled Struct.* **2024**, *200*, 111894. [CrossRef]
8. Zhao, L.Y.; Yang, X.W. Improved frequency-domain spectral element method for vibration analysis of nonuniform pipe conveying fluid. *Thin-Walled Struct.* **2023**, *182*, 110254. [CrossRef]
9. Khazaee, M.; Khadem, S.E.; Moslemi, A.; Abdollahi, A. Vibration mitigation of a pipe conveying fluid with a passive geometrically nonlinear absorber: A tuning optimal design. *Commun. Nonlinear Sci. Numer. Simul.* **2020**, *91*, 105439. [CrossRef]
10. Iqbal, M.; Jaya, M.M.; Savadkoohi, A.T.; Baguet, S. Vibration attenuation of dual periodic pipelines using nterconnected vibration absorbers. *Eng. Struct.* **2025**, *322 Pt A*, 11904.
11. Liu, Z.; Tan, X.; Liu, X.; Chen, P.; Yi, K.; Yang, T.Z.; Ni, Q.; Wang, L. Dynamical stability of cantilevered pipe conveying fluid with inerter-based dynamic vibration absorber. *Comput. Model. Eng. Sci.* **2020**, *125*, 495–514. [CrossRef]
12. Pourmohammadi, M.J.; Eftekhari, M. Vibration suppression of pipe conveying fluid using a nonlinear absorber in longitudinal direction. *Appl. Ocean Res.* **2023**, *141*, 103797. [CrossRef]
13. Yang, F.; Sedaghati, R.; Esmailzadeh, E. Vibration suppression of structures using tuned mass damper technology: A state-of-the-art review. *J. Vib. Control* **2022**, *28*, 812–836. [CrossRef]
14. Kwag, S.; Eem, S.; Kwak, J.; Lee, H.; Oh, J.; Koo, G.H. Mitigation of seismic responses of actual nuclear piping by a newly developed tuned mass damper device. *Nucl. Eng. Technol.* **2021**, *53*, 2728–2745.
15. Kwag, S.; Eem, S.; Kwak, J.; Lee, H.H.; Oh, J.; Koo, G.H.; Chang, S.J.; Jeon, B.G. Experimental study on seismic responses of tuned mass damper-applied real-scale piping system via shaking table tests. *Structures* **2023**, *50*, 1625–1652. [CrossRef]
16. Philip, R.; Santhosh, B.; Balaram, B.; Awrejcewicz, J. Vibration control in fluid conveying pipes using NES with nonlinear damping. *Mech. Syst. Signal Process.* **2023**, *194*, 110250. [CrossRef]
17. Mamaghani, A.E.; Khadem, S.E.; Bab, S. Vibration control of a pipe conveying fluid under external periodic excitation using a nonlinear energy sink. *Nonlinear Dyn.* **2016**, *86*, 1761–1795. [CrossRef]
18. Mirhashemi, S.; Saeidiha, M.; Ahmadi, H. Dynamics of a harmonically excited nonlinear pipe conveying fluid equipped with a local nonlinear energy sink. *Commun. Nonlinear Sci. Numer. Simul.* **2023**, *118*, 107035. [CrossRef]
19. Aloschi, F.; Andreotti, R.; Bursi, O.S. Pipe vibration attenuation through internal damping and optimal design of vibro-impact systems. *Sci. Rep.* **2023**, *13*, 6510. [CrossRef]

20. Pellizzari, F.; Marano, G.C.; Palmeri, A.; Greco, R.; Domaneschi, M. Robust optimization of MTMD systems for the control of vibrations. *Probabilistic Eng. Mech.* **2022**, *70*, 103347. [CrossRef]
21. Alehashem, S.M.S.; Wang, J.; Ni, Y.Q.; Keyhani, A. Vibration control of structures against near-field earthquakes by using a novel hydro-pneumatic semi-active resettable device. *Strucut. Control Health Monit.* **2022**, *29*, e3054.
22. Wang, L.K.; Nagarajaiah, S.; Shi, W.X.; Zhou, Y. Seismic performance improvement of base-isolated structures using a semi-active tuned mass damper. *Eng. Struct.* **2022**, *271*, 114963. [CrossRef]
23. Kumar, P.; Jangid, R.S.; Reddy, G.R. Response of piping system with semi-active variable stiffness damper under tri-directional seismic excitation. *Nucl. Eng. Des.* **2013**, *258*, 130–143. [CrossRef]
24. Bhaiya, V.; Bharti, S.D.; Shrimali, M.K.; Datta, T.K. Hybrid seismic control of buildings using tuned mass and magnetorheological dampers. *Proc. Inst. Civ. Eng.—Struct. Build.* **2020**, *173*, 471–487. [CrossRef]
25. Weber, F. Semi-active vibration absorber based on real-time controlled MR damper. *Mech. Syst. Signal Process.* **2014**, *46*, 272–288. [CrossRef]
26. Weber, F.; MasLanka, M. Frequency and damping adaptation of a TMD with controlled MR damper. *Smart Mater. Struct.* **2012**, *21*, 55011–55027. [CrossRef]
27. Maslanka, M. Optimised semi-active tuned mass damper with acceleration and relative motion feedbacks. *Mech. Syst. Signal Process.* **2019**, *130*, 707–731. [CrossRef]
28. Ghadimi, B.; Taghikhany, T. Dynamic response assessment of an offshore jacket platform with semi-active fuzzy-based controller: A case study. *Ocean. Eng.* **2021**, *238*, 109747. [CrossRef]
29. Gong, F.; Nie, S.; Ji, H.; Hong, R.; Yin, F.; Yan, X. Pipeline vibration control using magnetorheological damping clamps under fuzzy–PID control algorithm. *Micromachines* **2022**, *13*, 531. [CrossRef]
30. Jin, J.; Song, Z. Parametric resonances of a pipe conveying fluid and their numerical simulations. *J. Shenyang Inst. Aeronaut. Eng.* **2003**, *20*, 1–4.
31. Sternberg, A.; Zemp, R.; Llera, J.C.D.L. Multiphysics behavior of a magneto-rheological damper and experimental validation. *Eng. Struct.* **2014**, *69*, 194–205. [CrossRef]
32. Christopher, B. Simulating Viscous Heating in a Fluid Damper. Available online: https://www.comsol.com/blogs/simulating-viscous-heating-in-a-fluid-damper (accessed on 1 February 2025).
33. Zheng, J.; Li, Y.; Li, Z.; Wang, J. Transient multi-physics analysis of a magnetorheological shock absorber with the inverse Jiles-Atherton hysteresis model. *Smart Mater. Struct.* **2015**, *24*, 105024. [CrossRef]
34. Modeling and Simulation of MR Dampers Using COMSOL Multiphysics® Software. Available online: https://cn.comsol.com/paper/modeling-and-simulation-of-mr-dampers-using-comsol-multiphysics-software-19805 (accessed on 1 February 2025).
35. Yu, M.; Wang, S.Q.; Fu, J.; Peng, Y.X. Unsteady flow damping force prediction of MR dampers subjected to sinusoidal loading. *J. Phys. Conf. Ser.* **2013**, *412*, 012052. [CrossRef]
36. Spencer, B.; Dyke, S.; Sain, M.K.; Carlson, J.D. Phenomenological model of a magnetorheological damper. *J. Eng. Mech.* **1996**, *123*, 1–23. [CrossRef]
37. Wang, J. *Advanced Nonlinear Control Theory and Its Applications*; Science Press: Beijing China, 2012.
38. Simulink Online—MATLAB & Simulink (mathworks.cn). Available online: https://ww2.mathworks.cn/products/simulink-online.html (accessed on 12 February 2025).
39. Kandil, M.; El-Sayed, T.A.; Kamal, A.M. Unveiling the impact of pipe materials on water hammer in pressure pipelines: An experimental and numerical study. *Sci. Rep.* **2024**, *14*, 30599. [CrossRef] [PubMed]

Disclaimer/Publisher's Note: The statements, opinions and data contained in all publications are solely those of the individual author(s) and contributor(s) and not of MDPI and/or the editor(s). MDPI and/or the editor(s) disclaim responsibility for any injury to people or property resulting from any ideas, methods, instructions or products referred to in the content.